COMPARISON OF TWO K-ϵ MODELS FOR SIMULATION OF TURBULENT NATURAL CONVECTION IN A SQUARE CAVITY

C. BEGHEIN, C. INARD, F. ALLARD
Centre de Thermique de l'INSA de Lyon, URA CNRS 1372
INSA, bât. 307, 20 av. A. Einstein,
69621 Villeurbanne, France.

ABSTRACT

Turbulent natural convection in a square cavity filled with air and submitted to horizontal temperature gradients is studied numerically. Turbulence is modelled using k-ϵ models, the resulting differential equations are solved with SIMPLER algorithm. Two distinct k-ϵ models are compared. The former is derived from the well known "high Reynolds number k-ϵ model": the constants of this model are identical to ones usually used; nevertheless, the boundary conditions are not expressed on the first internal node out of the viscous boundary layer, but at the wall. The latter is a "low Reynolds number model" based on a previous work of Abrous et al.. The low Reynolds number effects are modelled using the turbulent viscosity concept defined as a function of the local turbulent Reynolds number, and the mesh includes the viscous sublayers.

KEYWORDS Turbulence, k-ϵ Model, Convection

INTRODUCTION

The aim of this study is to compare the behaviors of two different k-ϵ models, for case of convection in a thermally driven square cavity. A first series of results obtained with the reference standard k-ϵ model proposed by Prof. C.J. Hoogendoorn and dr. R.A.W.M. Henkes enables us to validate our code. This model is then compared to the low-Reynolds number k-ϵ model proposed by Abrous et al..

PHYSICAL AND MATHEMATICAL MODELS

Physical model

The physical model to be studied here is a square cavity filled with air whose upper and lower horizontal walls are adiabatic, vertical walls are submitted to constant temperature levels. The fluid motion is induced by the temperature difference between the left hot wall and the right cold one.

Mathematical model

The turbulent behavior of fluid is modelled via the eddy viscosity concept proposed by Boussinesq which relates the turbulent stresses $-\overline{u'_i u'_j}$ to the mean velocity gradients. The turbulent heat fluxes $-\overline{u'_j T'}$ are expressed from Reynolds analogy between momentum and heat. The turbulent viscosity is calculated in each point of the cavity from the two-equation k-ϵ model of turbulence. The resulting equations written in their dimensionless form are the following:

Continuity

$$\frac{\partial \overline{u_i}}{\partial x_i}=0 \tag{1}$$

Momentum

$$\overline{u_j}\frac{\partial \overline{u_i}}{\partial x_j}=-\frac{\partial \overline{P}}{\partial x_i}+\frac{1}{Gr^{1/2}}\frac{\partial}{\partial x_j}\left[(1+\nu_t)\frac{\partial \overline{u_i}}{\partial x_j}\right] + \frac{1}{Gr^{1/2}}\frac{\partial}{\partial x_j}\left[(1+\nu_t)\frac{\partial \overline{u_j}}{\partial x_i}\right]+\delta_{i2}g\beta(\overline{T}-0.5)-\frac{2}{3}\frac{\partial k}{\partial x_i} \tag{2}$$

Energy

$$\overline{u_j}\frac{\partial \overline{T}}{\partial x_j}=\frac{1}{Gr^{1/2}}\frac{\partial}{\partial x_j}\left[\left(\frac{1}{Pr}+\frac{\nu_t}{\sigma_T}\right)\frac{\partial \overline{T}}{\partial x_j}\right] \tag{3}$$

Turbulent kinetic energy

$$\overline{u_j}\frac{\partial k}{\partial x_j}=\frac{1}{Gr^{1/2}}\frac{\partial}{\partial x_j}\left[\left(1+\frac{\nu_t}{\sigma_k}\right)\frac{\partial k}{\partial x_j}\right] + \frac{1}{Gr^{1/2}}(P_k+G_k)-\epsilon \tag{4}$$

Dissipation rate of turbulent kinetic energy

$$\overline{u_j}\frac{\partial \epsilon}{\partial x_j}=\frac{1}{Gr^{1/2}}\frac{\partial}{\partial x_i}\left[\left(1+\frac{\nu_t}{\sigma_\epsilon}\right)\frac{\partial \epsilon}{\partial x_i}\right] + \frac{1}{Gr^{1/2}}\left(C_{\epsilon 1}f_1(P_k+C_{\epsilon 3}G_k)\right)\frac{\epsilon}{k}-C_{\epsilon 2}f_2\frac{\epsilon^2}{k} \tag{5}$$

Turbulent viscosity

$$\nu_t=Gr^{1/2}C_\mu f_\mu\frac{k^2}{\epsilon} \tag{6}$$

With:

$$P_k=\frac{1}{Gr^{1/2}}\frac{\nu_t}{2}\left(\frac{\partial\overline{u_i}}{\partial x_j}+\frac{\partial\overline{u_j}}{\partial x_i}\right)^2 \tag{7}$$

$$G_k=-\frac{1}{Gr^{1/2}}\frac{\nu_t}{\sigma_T}\frac{\partial\overline{T}}{\partial x_j}\delta_{j2} \tag{8}$$

The non-dimensional variables are:

$$\begin{aligned} &x_i=x^*_i/H;\ u_i=u^*_i/u_0 \\ &T=(T^*-T_C)/(T_H-T_C)\ ;\ P=P^*/(\rho u_0)^2 \\ &k=k^*/u_0^2;\ \epsilon=\epsilon^*/(u_0^3/H)\ ;\ \nu_t=\nu_t^*/\nu \end{aligned} \tag{9}$$

As the buoyancy process is much stronger than the diffusion process for turbulent flows, the velocities are made dimensionless with the buoyant velocity u_0:

$$u_0=(g\beta\Delta TH)^{1/2} \tag{10}$$

In this study, 2 k-ϵ models are investigated:

1. High Reynolds number k-ϵ model proposed by Henkes and Hoogendoorn in Eurotherm-Ercoftac Workshop (Henkes 1989)
2. Low Reynolds number k-ϵ model developed by Abrous et al. (1984)

In the standard k-ϵ model, no wall functions are used in order to obtain grid independent results for the turbulent quantities; indeed, the dissipation rate of turbulent kinetic energy is set infinite at the wall. $C_{\epsilon 1}f_1$, $C_{\epsilon 2}f_2$, $C_\mu f_\mu$ are constant within the whole flow domain. These constants, the turbulent Prandtl numbers and the boundary condition for ϵ are the following:

$$\begin{aligned} &C_{\epsilon 1}f_1=1.44;\ C_{\epsilon 2}f_2=1.92;\ C_{\epsilon 3}=tanh\left|\frac{\overline{v}}{\overline{u}}\right|;\ C_\mu f_\mu=.09 \\ &\sigma_T=0.9;\ \sigma_k=1.0;\ \sigma_\epsilon=1.3 \\ &\epsilon_{wall}=\infty \end{aligned} \tag{11}$$

Low Reynolds modelling consists in using damping functions f_1, f_2, f_μ, rather than constants, to account for the laminar behavior of fluid close to the walls. Hence, the first discretization node is located within the viscous sublayer.

In the model developed by Abrous et al., the values of $C_{\epsilon 1}f_1$, $C_{\epsilon 2}f_2$, $C_\mu f_\mu$, σ_T, σ_k, σ_ϵ are as recommended by Launder and Spalding (1974):

$$\begin{aligned} &C_{\epsilon 1}f_1=1.44,\ C_{\epsilon 2}f_2=1.92 \\ &C_\mu f_\mu=.09\,exp[-3.4/(1+R_t/50)^2]\ \ where\ R_t=Gr^{1/2}k^2/\epsilon \\ &\sigma_T=1.0,\ \sigma_k=1.0,\ \sigma_\epsilon=1.3 \end{aligned} \tag{12}$$

In order to take into account the viscous effects in the viscous sublayer, f_μ depends on

the local turbulence Reynolds number R_t. $C_{\epsilon 3}$, which is .4 near horizontal walls and 1.44 near vertical walls, is assigned the following value:

$$C_{\epsilon 3} = .7 + (1.44 - .7) \frac{|\overline{u}|}{\sqrt{\overline{u^2} + \overline{v^2}}} \qquad (13)$$

The boundary condition for ϵ is deduced from the expression of the balance of k in the viscous sublayer (To and Humphrey 1986):

$$\epsilon_{wall} = \frac{2}{Gr^{1/2}} \left(\frac{\partial k^{1/2}}{\partial x} \right)^2_{wall} \qquad (14)$$

For these two models, the turbulent kinetic energy is zero at the wall.

NUMERICAL METHOD

The equations to be solved are advection-diffusion equations, coupled with pressure, velocities, temperature and turbulent quantities. They are spatially discretized over a staggered grid by the finite difference method and then integrated over control volumes. The system of equations is implicitly solved by the SIMPLER (Semi Implicit Method for Pressure Linked Equations Revised) iterative process proposed by Patankar (1980). The equations are discretized with the Power-Law scheme. The solution option of the finite difference equations is the line by line Tri-Diagonal Matrix Algorithm (TDMA) (Anderson et al. 1983). Special attention is paid to the implicit under-relaxation of the set of equations, the explicit under-relaxation of the turbulent quantities, and to the k and ϵ equations source terms linearization. Convergence of the SIMPLER algorithm is reached when the residuals of all the equations are very small.

RESULTS & DISCUSSION

Qualitative results obtained with the standard k-ϵ model are presented. Simulations were carried out, for a Rayleigh number range between 10^8 and 10^{12}. Streamlines and isopleths of temperature and turbulent viscosity are plotted in figures 1,2,3. In the core of the cavity, a stratification of temperature pattern is to be noticed. The size of this area increases with Rayleigh number, while the thermal boundary layer thickness decreases (figures 2.a, 2.b, 2.c). So does the dynamic boundary layer thickness; the hydraulic jump which occurs for low Rayleigh numbers (figure 1.a) disappears for higher Rayleigh numbers (figures 1.b, 1.c): the higher the Rayleigh number, the higher the turbulent viscosity, the stronger the diffusion process. The behavior of the fluid is turbulent in the top left and bottom right parts of the cavity, these areas strech along the horizontal walls, when Rayleigh number is increased (figures 3.a, 3.b, 3.c).

The values of the average Nusselt number at hot wall and the maximum vertical velocity at half the cavity height, obtained with the two k-ϵ models, and for different Rayleigh numbers, were computed. These results highlight the different behaviors of the standard k-ϵ model and the low Reynolds number k-ϵ model proposed by Abrous et al.. From Figure 4, it is seen that the transition region between the laminar and the turbulent behaviors differs. The transition occurs at $Ra = 10^9$ for the standard model and at $Ra = 10^{10}$ for Abrous low Reynolds number model. The slopes of the curves in the

turbulent regime are not the same; the standard model overpredicts the average heat transfer rate at hot wall. Maximum values of the non dimensional vertical velocity at mid height of the cavity are plotted in Figure 5. Although the two models predict identical values for the laminar regime ($Ra=10^8$), a great discrepancy is to be noticed for the maximum vertical velocity at the laminar-turbulent transition. In the turbulent regime, the values of non dimensional vertical velocity decrease and get closer for both models.

CONCLUSIONS

Turbulent natural convection in a thermally driven square cavity was numerically investigated. A standard k-ϵ model with boundary conditions for turbulent quantities imposed at the wall and a low Reynolds number k-ϵ model were used. The numerical procedure is the SIMPLER algorithm. Discrepancies between the two models are to be noticed, for prediction of significant quantities such as the average Nusselt number at hot wall, or the maximum vertical velocity at half the cavity height. Moreover, the laminar-turbulent transition region, for different values of Rayleigh numbers, is not the same for both models. Other results by direct simulations or experiments need therefore to be performed, in order to predict the turbulent motion with a more accurate turbulence model.

REFERENCES

A. ABROUS, A.F. EMERY, F. KAZEMZADEH, "Turbulent free convection in rooms in presence of drafts, cold windows and solar radiation", Heat transfer in enclosures, ASME winter annual meeting, New Orleans, Louisiana, HTD vol.39, pp. 49-54 (1984).

D.A. ANDERSON, J.C. TANNEHILL, R.H. PLETCHER, "Computational fluid mechanics and heat transfer", Hemisphere, Washington (1983).

R.A.W.M. HENKES, "Natural convection boundary layers", PhD thesis, Delft University of Technology, Faculty of Applied Physics, The Netherlands (1989).

B.E. LAUNDER, D.B. SPALDING, "Numerical computation of turbulent flows", Computer Methods in Applied Mechanics and Engineering, vol.3, pp. 269-289, North-Holland (1974).

S.V. PATANKAR, "Numerical heat transfer and fluid flow", Mac Graw Hill, London (1980).

W.M. TO, J.A.C. HUMPHREY, "Numerical simulation of buoyant, turbulent flow - 1. Free convection along a heated, vertical, flat plate", Int. J. Heat Mass Transfer, vol.29, no 4, pp. 573-592 (1986).

ACKNOWLEDGEMENTS

Calculations were performed on the IBM 3090 supercomputer of the CNUSC (Centre National Universitaire Sud de Calcul) of Montpellier (France), within the frame of the C3NI (Centre de Compétence en Calcul Numérique Intensif).

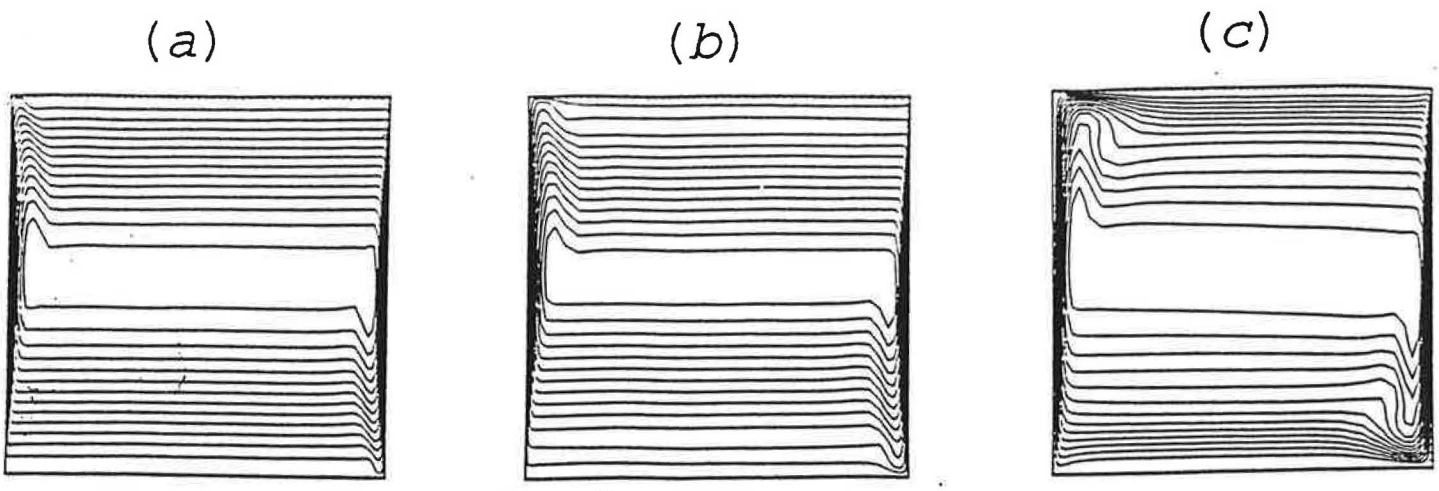

Figure 1 *Streamlines*
(a) Ra = 10^8, (b) Ra = 10^{10}, (c) Ra = 10^{12}

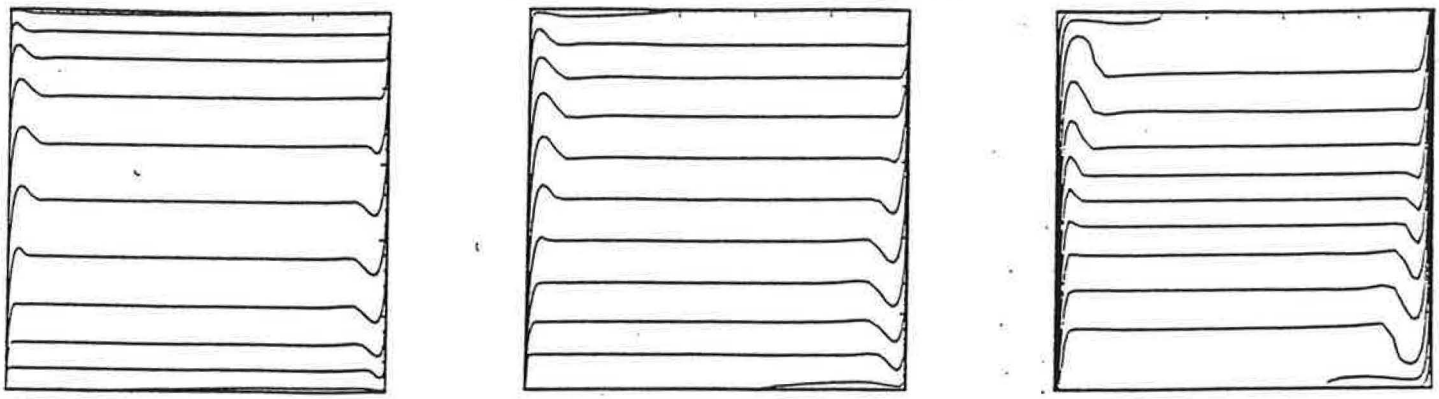

Figure 2 *Isopleths of temperature*
(a) Ra = 10^8, (b) Ra = 10^{10}, (c) Ra = 10^{12}

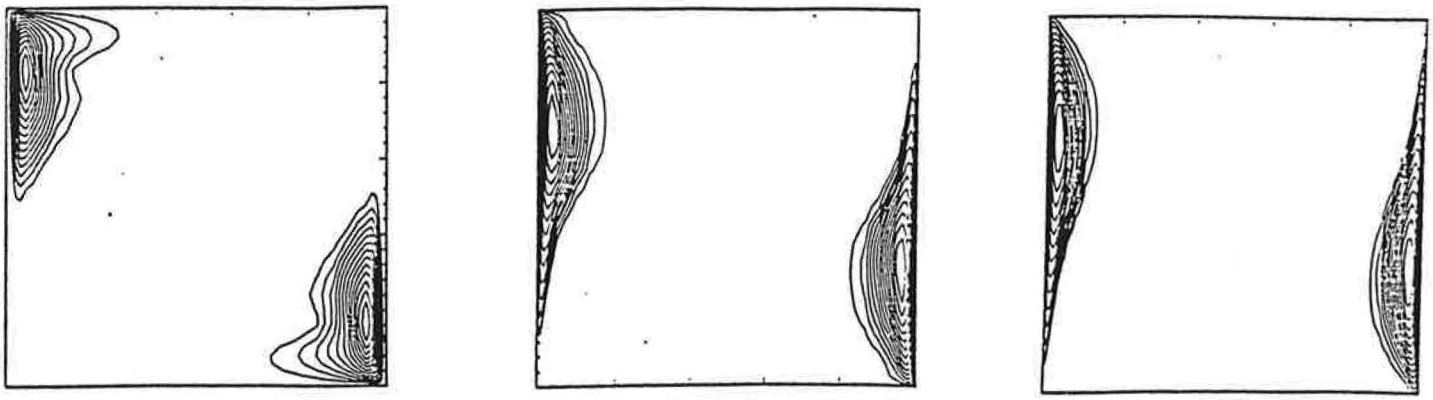

Figure 3 *Isopleths of turbulent viscosity*
(a) Ra = 10^8, (b) Ra = 10^{10}, (c) Ra = 10^{12}

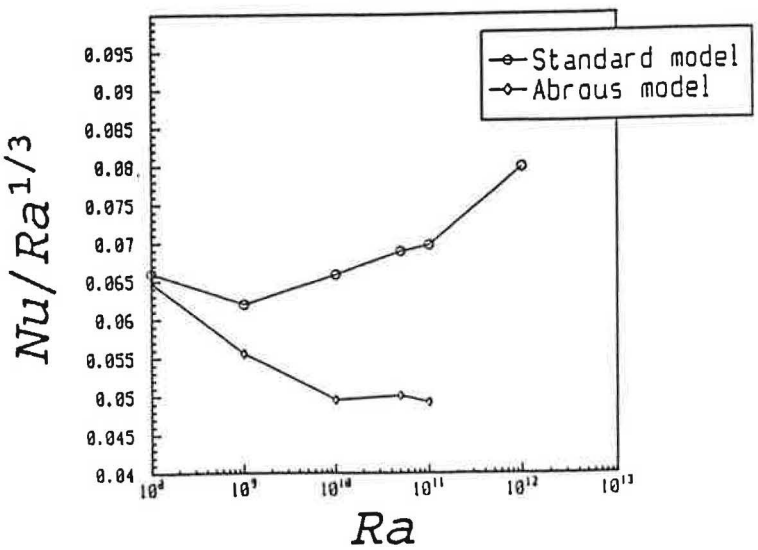

Figure 4 *Average Nusselt number at hot wall*

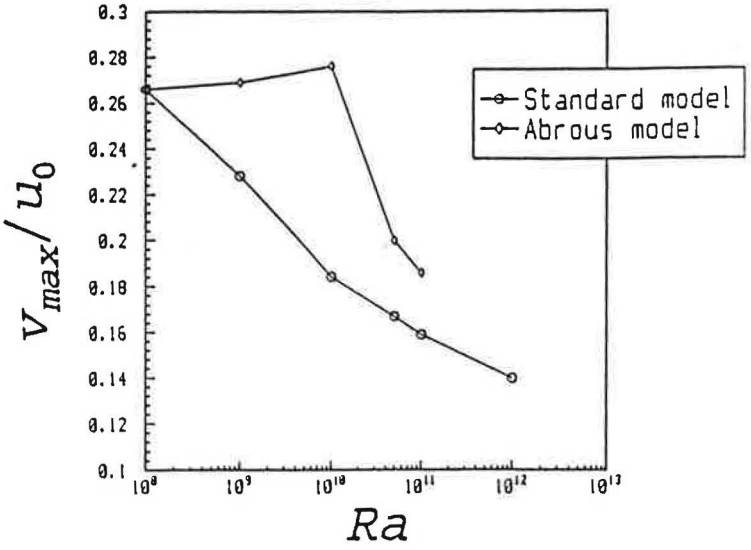

Figure 5 *Maximum vertical velocity at mid height of the cavity*

International Symposium on Room Air Convection and Ventilation Effectiveness
University of Tokyo, July 22 – 24, 1992

LOW-IMPULSE CEILING DIFFUSOR FOR DISPLACEMENT VENTILATION

Bjørn Kvisgaard
Brüel & Kjær
Nærum, Denmark

Jørgen Schmidt Madsen
Lindab-Riscanco
Farum, Denmark

ABSTRACT

The past few years have seen a wide-spread use of displacement ventilation for room ventilation. The principle has several advantageous characteristics, of which special attention has been paid to its possibilities of more efficient use of the ventilation air for cooling of workplaces and removal of pollutants. The arguments against the use of displacement ventilation are primarily that the installation of the wall-mounted air outlet devices is expensive; that draught problems may arise close to the outlet; and that the ventilation principle seldomly works when only small air quantities are to be supplied to the room.

We shall examine a system layout where the air is supplied through low-impulse air outlet devices mounted in the ceiling. The philosophy of the this layout is that the cold air is "poured" into the room at a spot not normally used for occupation, e.g. close to the door. On its way to the floor the supply air will be mixed with room air, and as it reaches the floor the amount and temperature of the supply air should be sufficient for ventilation of the rest of the room by the displacement principle. If the examined ventilation system proves to work as described, it will be an inexpensive system for comfort ventilation using the displacement principle.

The tests are carried out as laboratory tests under controlled conditions, with complete recording of all relevant parameters, such as temperature, air velocity, age-of-air in the occupied zone, and air-exchange efficiency in the room. Heated manikins are used to simulate influence of occupants.

KEYWORDS Low-impulse, ceiling diffusor, age-of-air

INTRODUCTION

Testing new principles of ventilation is a huge task involving numerous calculations and experiments. The work we have conducted is only to be considered a preliminary investigation with the purpose of getting an impression of the advantages and disadvantages of the low-impulse ceiling supply principle.

We have chosen to conduct the investigation as a comparative investigation with three different air supply principles. Low-impulse ceiling diffusion will be compared to Normal mixing ventilation and Displacement ventilation.

The tests were made in a 33 m^2 office room, specially made for this purpose, with four workplaces. A heated manikin (100 W) as well as a heated computer-screen dummy (100 W) were placed at each workplace. Figure 1 shows a plan of the room.

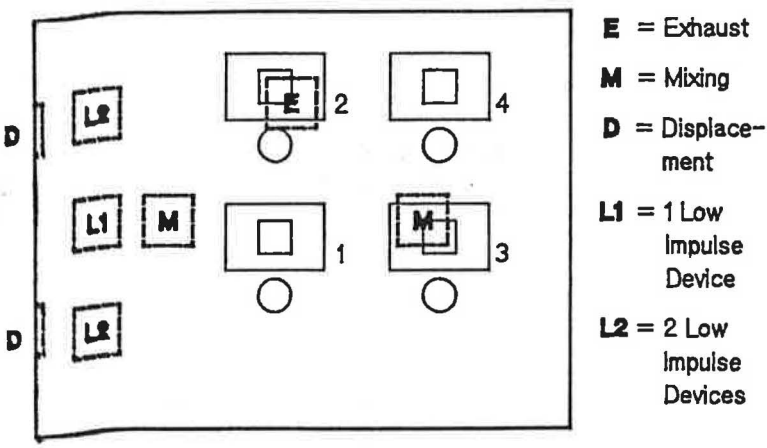

Fig. 1 Plan of test room, showing the location of the four workplaces, and the air inlet and outlet devices. The two devices for displacement ventilation are placed in the side wall at floor level, while the others are built into the ceiling

The height of the test room is 2.6 m. Apart from persons and computer screens there is a slight thermal load (224 W) from the electrical light, and minor heat exchange with the surrounding rooms.

ADJUSTMENT OF LOW-IMPULSE AIR OUTLET DEVICES

Supply of cold air with low impulse, from a ceiling diffusor may cause some problems, since the air stream from the outlet tends to converge on its way towards the floor.

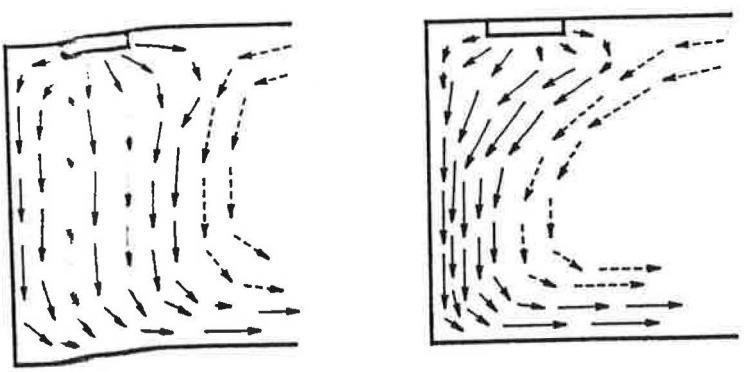

Fig. 2 Shape of air stream at supply from ceiling-mounted low-impulse air outlet. The full-drawn lines show the flow from the air outlet and the dotted lines show the movement of the room air.

Parameters deciding the shape of the air stream are temperature difference and injection velocity. Figure 2 shows the two shapes of the air stream observed during adjustment of the air outlet diffusors.

During the tests the air outlet device has been adjusted to achieve a diffusing air stream. The normal circulation of room air is controlled by the air supply as well as by the convective air currents around the heat sources. In the test set up the two forces work together and create a vortex circulating around a horizontal axis across the room. This vortex will try to press the supply air stream up against the end wall. Therefore, a certain impulse in the supply air is necessary to overcome the vortex forces.

AIR DISTRIBUTION IN THE ROOM

The air distribution and the air exchange efficiency were measured with tracer gas using the age-of-air method. In short, the method involves measuring the time it takes the air to get from the air supply to a number of measurement points in the room. One way of conducting the measurement is to mark all supply air with tracer gas from the time zero, and then monitor how fast the marked air reaches the measurement points.

We have chosen to measure local mean age-of-air in four points in the room and in the air extraction duct. Furthermore, from the measurement in the air extraction we determine the room-average age-of-air and the air-exchange efficiency. We use the European scale for air-exchange efficiency, where a piston flow gives the value 100%, full mixture gives the value 50%, and short-circuit gives values less than 50%.

Measurement no.	1-4	5-8	9-12	14-15	16-19	20-21
Type	Low 1	Disp.	Mix.	Low 2	Mix.	Disp.
Local mean age:						
Desk 2, 0.6 m (4)	565	308	634	530	653	402
Desk 2, 1.1 m (6)	582	410	643	597	654	477
Desk 2, 1.7 m (5)	606	516	624	605	642	731
Desk 3, 1.1 m (1)	587	327	677	585	703	358
Exhaust (3)	628	575	528	603	554	581
Room-average age-of-air	607	480	698	573	714	504
Air-exchange eff.	51%	60%	38%	53%	39%	58%
Temp. supply C	15.2	15.2	15.0	17.0	17.1	17.1
Temp. extract C	21.7	22.2	21.0	22.1	22.4	22.4
Heat removed kW	1.10	1.20	1.05	0.86	0.90	0.90

Table 1 Results for measurements of age-of-air and thermal load for the three ventilation systems. All age-of-air results are in seconds. "Low 1" indicates that the supply air has been injected through the middle low-impulse ceiling diffuser. "Low 2" indicates that the two outermost low-impulse ceiling diffusers have been used. The air-exchange in the room during measurements was between 540 and 560 m3/h. Leakage from the room to the surroundings constitute 5-10% of the total air-exchange of the room.

Figure 3 shows typical step-up curves for the three principles of ventilation and Table 1 lists the key figures for the three principles, to facilitate comparison.

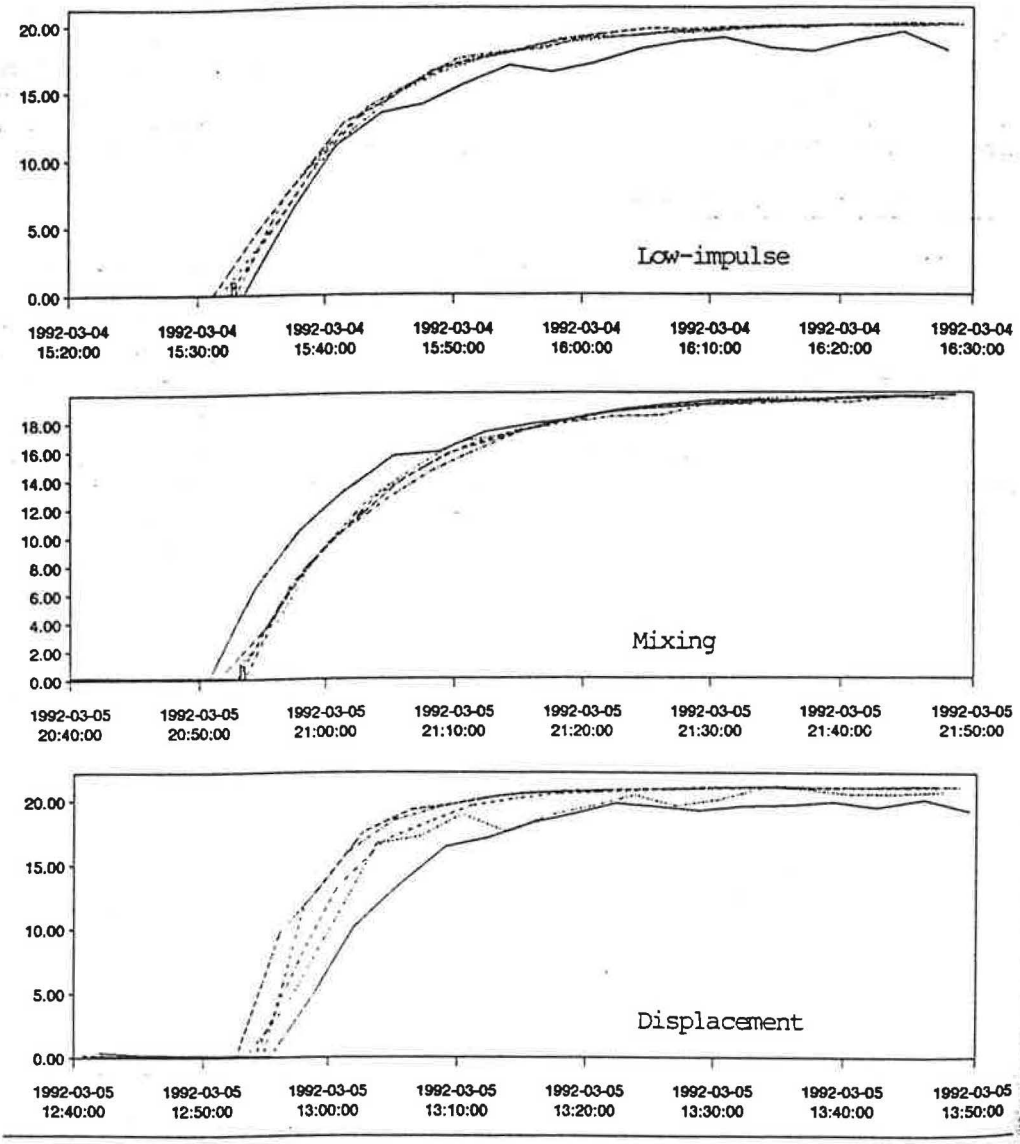

C	Location:	Measurement	Line	Scale	Unit	Room Vol.
3	Exhaust	Sulphur Hexaf.	——	1E+00	ppm	86.50 m^3
4	Desk2, 0.6m	Sulphur Hexaf.	----	1E+00	ppm	86.50 m^3
5	Desk2, 1.7m	Sulphur Hexaf.	----	1E+00	ppm	86.50 m^3
1	User Index 1	Marker	ıı	1E+00		None
1	Desk3, 1.1m	Sulphur Hexaf.	——	1E+00	ppm	86.50 m^3
6	Desk2, 1.1m	Sulphur Hexaf.	----	1E+00	ppm	86.50 m^3

Fig. 3 Step-up curves for measuring age-of-air for low-impulse ceiling diffuser, mixing ventilation, and displacement ventilation. "Marker" indicates the point of time where the tracer-gas dosing started.

THERMAL COMFORT

In order to evaluate the thermal comfort at the different principles of ventilation, temperature and air velocity were measured at a number of points in the room.

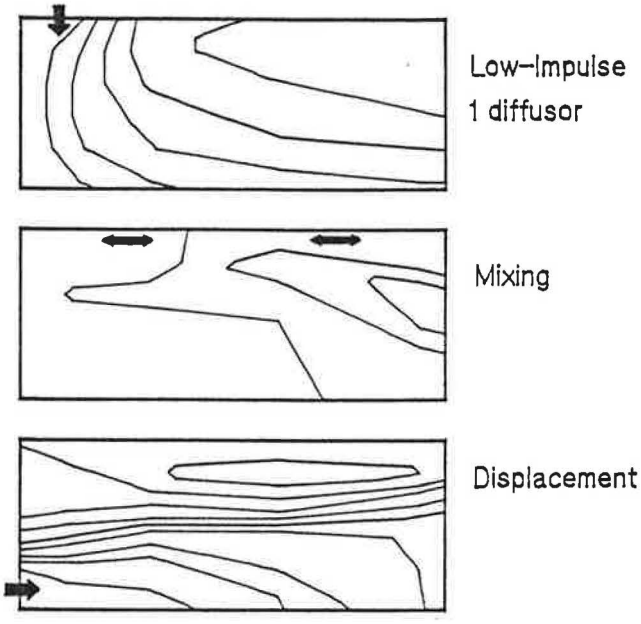

Fig. 4 Isotherms in a sectional elevation across the room for the three different principles of ventilation. The distance between the isotherms is 0.5 °C.

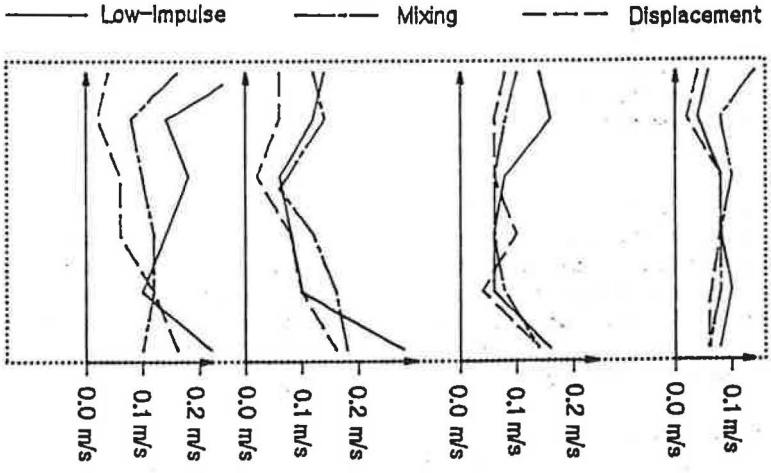

Fig. 5 Mean air velocity in four vertical lines in a sectional elevation across the room. The dotted line shows the contour of the room. The measurements are carried out at distance 0.7 m, 2.0 m, 4.0 m and 6.2 m from the left wall. At each point measurements are done in the heights 0.1 m, 0.6 m, 1.1 m, 1.6 m, 2.1 m and 2.5 m. Outlet devices for low-impulse ceiling supply and displacement ventilation are situated in the left side of the room.

The sensation of draught is a function of both mean air velocity, turbulence intensity and air temperature. Therefore, Figure 5 does not show directly the number of persons feeling draught. The percentage of dissatisfied can be calculated by the equations in /1/.

Among the measurement points shown in Figure 5, it is the point 0.1 m above the floor and 2.0 m from the left end wall that creates most draught. The percentage of dissatisfied for that point will be as follows:

Mixing ventilation	16% dissatisfied
Displacement ventilation	15% dissatisfied
Low-impulse with 1 diffuser	26% dissatisfied
Low-impulse with 2 diffusers	19% dissatisfied

Control measurements at other points in the room did not reveal points with thermal conditions worse than as shown above.

CONCLUSION

The measurements we have performed do not directly indicate whether the use of low-impulse ceiling diffusers is a good idea or not. There are a number of problems about this principle of ventilation, but also some advantages; just as the principles of ventilation used in the comparison have advantages and disadvantages.

The main problem of the low-impulse ceiling supply is that it accelerate a too big air volume. The result being that the air velocities in the occupied zone are too high and that the displacing effect does not occur. Injection with two diffusors will give better results than injection with one diffusor, and it is probably the air supply diffusors that need development in order to improve results with this principle of ventilation. It is imperative that the air supply diffusors are able to disperse the supply air without triggering off too much movement of air.

The largest problem of the mixing ventilation is a very small air-exchange efficiency. More than 20% of the supply air goes dicrectly from the supply to the extract without entering the occupied zone at all. The reason for this short-circuit is the location of the exhaust

In the case of perfect mixing the location of the extract does not matter at all, but perfect mixing does not exist in real life. Judging from the air velocities and air flow pattern in the occupied zone we can estimate that the room air is circulated approx. 20 times an hour. Since the fresh-air exchange is 6.7 times an hour, 30% of the air is exchanged every time it passes the ceiling. The location of supply and extract in relation to the general direction of flow is therefore very critical.

Displacement ventilation gives a satisfactory air flow through the room. On the comfort side the large temperature gradient in the room may cause problems. This may be remedied by injection of larger amounts of air with less temperature difference.

REFERENCES

/1/ Fanger, P.O., Melikov, A.K., Hanzawa, H., Ring, J. "Air turbulence and sensation of draught". Energy and Buildings, 12, 1, 1988, pp...